

# Exploration of decaying dark matter in a left-right symmetric model

Wan-Lei Guo,<sup>\*</sup> Yue-Liang Wu,<sup>†</sup> and Yu-Feng Zhou<sup>‡</sup>

*Kavli Institute for Theoretical Physics China,*

*Key Laboratory of Frontiers in Theoretical Physics,*

*Institute of Theoretical Physics, Chinese Academy of Science, Beijing 100190, China*

## Abstract

$SU(2)_L$  triplet scalars appear in models motivated for the left-right symmetry, neutrino masses and dark matter (DM), etc.. If the triplets are the main decay products of the DM particle, and carry nonzero lepton numbers, they may decay dominantly into lepton pairs, which can naturally explain the current experimental results reported by PAMELA and Fermi-LAT or ATIC. We discuss this possibility in an extended left-right symmetric model in which the decay of DM particle is induced by tiny soft charge-conjugation ( $C$ ) violating interactions, and calculate the spectra for cosmic-ray positrons, neutrinos and gamma-rays. We show that the DM signals in the flux of high energy neutrinos can be significantly enhanced, as the triplets couple to both charged leptons and neutrinos with the same strength. In this scenario, the predicted neutrino-induced muon flux can be several times larger than the case in which DM particle only directly decays into charged leptons. In addition, the charged components of the triplet may give an extra contribution to the high energy gamma-rays through internal bremsstrahlung process, which depends on the mass hierarchy between the DM particle and the triplet scalars.

PACS numbers: 95.35.+d, 98.70.Sa, 12.60.-i

---

<sup>\*</sup>Email: guowl@itp.ac.cn

<sup>†</sup>Email: ylwu@itp.ac.cn

<sup>‡</sup>Email: yfzhou@itp.ac.cn

## I. INTRODUCTION

Recently, the PAMELA satellite experiment has observed an excess in the positron fraction from 10 to 100 GeV [1], which confirmed the previous hints from HEAT [2], CAPRICE [3] and AMS-01 [4]. The reports from ATIC balloon experiment showed a rapid rise of the total electron and positron flux at a range 300-800 GeV[5] with a peak at around 600 GeV, which agreed with the PPB-BETS results[6]. More recently, the Fermi-LAT [7] and the HESS [8] Cherenkov experiments have released their results for the sum of electron and positron flux. Although they did not fully confirm the previous results reported by the ATIC experiment, both the measurements indicated excesses over the expected background, which suggests the presence of extra sources for the  $e^\pm$  spectra. Besides the astrophysical explanations for  $e^\pm$  anomalies by some nearby sources like pulsars and supernova remnants, the dark matter (DM) annihilation or decay is one of the most interesting explanation from particle physics.

The PAMELA, ATIC, and Fermi-LAT anomalies may be a consequence of DM particle annihilating mainly into lepton final states. However, if the dark matter is generated thermally, the annihilation cross section obtained from the observed relic density is significantly lower than that required by the current data. One has to resort to a large boost factor (about 100 – 1000) to explain the observed large positron flux. Note that the most probable boost factor from the clumpiness of DM structures is estimated to be less than  $\sim 10 - 20$  [9]. The large boost factor may come from nonperturbative Sommerfeld enhancement [10] or Breit-Wigner enhancement [11–13]. An other possibility is that the DM particle may slightly decay, and dominantly decay into leptons [14]. In this case the bound from the DM relic density is relaxed. The current data require that the lifetime of DM particle should be of the order  $\mathcal{O}(10^{26}\text{s})$ .

If the mass of DM particle is very heavy, it may first decay into some lighter intermediate states rather than directly into standard model (SM) particles. An interesting intermediate state might be  $SU(2)_L$  triplets, as it is known in many models that they may carry nonzero lepton numbers, and do not couple to quarks directly. This leptophilic feature can naturally account for the PAMELA results on both the excesses of positrons and the absence of large anti-proton flux.

The stability of the DM particle is usually protected by imposing extra discrete sym-

metries. In our previous work [15], we have shown that the fundamental symmetries of quantum field theory such as parity ( $P$ ) and charge-conjugation ( $C$ ) can be used to stabilize the DM particle. We have explicitly demonstrated that in a left-right (LR) symmetry model with  $P$  and  $CP$  only broken spontaneously, a gauge singlet scalar with odd  $CP$  parity can be automatically stable without imposing any extra discrete symmetries.

Motivated by the recent experimental results, we consider in this work the possibility of DM particle decay by adding soft  $C$ -violating interactions into our previous model, which will result in the decay of DM particle with  $SU(2)_L$  triplet scalars as intermediate states. The decays of the triplets into the SM gauge boson pairs  $W^\pm W^\pm$ ,  $W^\pm Z^0$ ,  $Z^0 Z^0$  as well as the SM-like Higgs bosons  $h^0 h^0$  are all suppressed by the smallness of the vacuum expectation value (VEV) of the left-handed triplet as required by the tiny neutrino masses. Thus the triplets decaying into quarks indirectly through these states are strongly suppressed.

If the reported positron excess indeed originates from DM particle decay through the intermediate  $SU(2)_L$  triplets, the possible associating signals such as the high energy neutrinos and gamma-rays are expected. This is because the neutral and singly charged components of the triplets couple to neutrinos in the same way as the doubly charged components couple to charged leptons. The final state leptons may generate high energy gamma-rays through inverse Compton scatterings (ICS) and final state radiations (FSR), which is common to many DM models. In this model the doubly and singly charged components of the triplet can also produce extra gamma-rays through virtual internal bremsstrahlung (VIB), which gives additional contributions to the gamma-ray spectrum at very high energy region.

In this work we first show how the DM particle decay caused by the soft  $C$ -violating interactions can naturally explain the observed excess of the positron and electron excesses, and then focus on the cosmic-ray signals associated with DM particle decay through intermediate  $SU(2)_L$  triplets in a LR symmetric model with two Higgs bidoublets [15, 16]. After exploring the typical parameters which can explain the current PAMELA as well as Fermi-LAT or ATIC data, we present predictions for the flux of neutrinos and gamma-rays. We find that the predicted neutrino-induced muon flux can be significantly larger than the case in which DM particle only directly decays into charged leptons. The energy spectrum of diffuse gamma-rays can be enhanced by the VIB processes from internal charged triplets as well. Although the analysis is done in a particular model, the conclusions are generally valid for other models which involve  $SU(2)_L$  triplets as intermediate states, such as the DM

models in connection to the type II seesaw mechanism for neutrino masses (see, e.g. Ref. [13]).

This paper is organized as follows: in Sec. II, we discuss the main features of the model and focus on the decay of DM particle induced by the soft  $C$ -breaking terms. In Sec. III, we calculate the DM decay signals which includes the positron fraction, total flux of electron and positron, neutrino-induced muon flux and high energy gamma-ray flux. The results are summarized in Sec. IV.

## II. DECAYING DARK MATTER IN A LR SYMMETRIC MODEL

We begin with a brief review of the LR model with two Higgs bidoublets described in Ref. [15, 16]. The model is a simple extension to the minimal LR model [17], which is based on the gauge group  $SU(2)_L \otimes SU(2)_R \otimes U(1)_{B-L}$ . The left- and right-handed fermions belong to the  $SU(2)_L$  and  $SU(2)_R$  doublets respectively. The Higgs sector contains two Higgs bidoublets  $\phi$  (2,2\*,0),  $\chi$  (2,2\*,0), a left(right)-handed Higgs triplet  $\Delta_{L(R)}$  (3(1),1(3),2), and a gauge singlet  $S$ (0,0,0) with the following flavor contents

$$\phi = \begin{pmatrix} \phi_1^0 & \phi_1^+ \\ \phi_2^- & \phi_2^0 \end{pmatrix}, \chi = \begin{pmatrix} \chi_1^0 & \chi_1^+ \\ \chi_2^- & \chi_2^0 \end{pmatrix}, \Delta_{L,R} = \begin{pmatrix} \delta_{L,R}^+/\sqrt{2} & \delta_{L,R}^{++} \\ \delta_{L,R}^0 & -\delta_{L,R}^+/\sqrt{2} \end{pmatrix}, S = \frac{1}{\sqrt{2}}(S_\sigma + iS_D). \quad (1)$$

The two triplets  $\Delta_{L,R}$  are responsible for breaking the left-right symmetry at high energy scale and generating small neutrino masses through the seesaw mechanism. The introduction of Higgs bidoublets  $\phi$  and  $\chi$  accounts for the electroweak symmetry breaking and overcome the fine-tuning problem in generating the spontaneous  $CP$  violation in the minimal LR model. Meanwhile it also relaxes the severe low energy phenomenological constraints. The gauge singlet  $S$  is relevant to the DM candidate.

The kinematic terms for the scalar fields are given by

$$\mathcal{L} = \text{Tr}[(D_\mu \phi)^\dagger (D^\mu \phi)] + \text{Tr}[(D_\mu \Delta_L)^\dagger (D^\mu \Delta_L)] + (\phi \leftrightarrow \chi, L \leftrightarrow R), \quad (2)$$

where

$$\begin{aligned} D_\mu \phi &= \partial_\mu \phi - ig \frac{\tau}{2} W_{L\mu} \phi + ig \phi \frac{\tau}{2} W_{R\mu}, \\ D_\mu \Delta_L &= \partial_\mu \Delta_L - ig \left[ \frac{\tau}{2} W_{L\mu}, \Delta_L \right] - ig' B_\mu \Delta_L. \end{aligned} \quad (3)$$

Due to constraints from low energy phenomenology, the mixing between  $W_L$  and  $W_R$  is rather small. Thus the SM gauge boson  $W^\pm$  is mostly  $W_L^\pm$ .

In this work, we shall focus on the scalar sector which is relevant to the DM particle. Under the  $P$  and  $CP$  transformations, the scalar fields transform as follows

	$P$	$CP$
$\phi$	$\phi^\dagger$	$\phi^*$
$\chi$	$\chi^\dagger$	$\chi^*$
$\Delta_{L(R)}$	$\Delta_{R(L)}$	$\Delta_{L(R)}^*$
$S$	$S$	$S^*$

(4)

The whole scalar potential contains two parts

$$\mathcal{V} = \mathcal{V}_0 + \mathcal{V}_1. \quad (5)$$

It is required that the dominant part  $\mathcal{V}_0$  is both  $P$ - and  $CP$ -invariant while a small part  $\mathcal{V}_1$  contains the soft  $C$ -violating interactions. The most general form for  $\mathcal{V}_0$  is given by [15]

$$\begin{aligned}
-\mathcal{V}_0 = & \frac{1}{\sqrt{2}}\tilde{\mu}_0^3(S+S^*) - \tilde{\mu}_S^2 SS^* - \frac{1}{4}\tilde{\mu}_\sigma^2(S+S^*)^2 + \sqrt{2}\tilde{\mu}_{\sigma S}(S+S^*)SS^* \\
& + \frac{1}{6\sqrt{2}}\tilde{\mu}_{3\sigma}(S+S^*)^3 + \tilde{\lambda}_S(SS^*)^2 - \frac{1}{4}\tilde{\lambda}_{\sigma S}(S+S^*)^2 SS^* - \frac{1}{16}\tilde{\lambda}_\sigma(S+S^*)^4 \\
& + \sum_{i=1}^5 \left[ -\frac{1}{\sqrt{2}}\tilde{\mu}_{i,\sigma}(S+S^*) + \tilde{\lambda}_{i,S}SS^* - \frac{1}{4}\tilde{\lambda}_{i,\sigma}(S+S^*)^2 \right] O_i,
\end{aligned} \quad (6)$$

where

$$\begin{aligned}
O_1 &= \text{Tr}(\Delta_L^\dagger \Delta_L + \Delta_R^\dagger \Delta_R), O_2 = \text{Tr}(\phi^\dagger \phi), O_3 = \text{Tr}(\phi^\dagger \tilde{\phi} + \tilde{\phi}^\dagger \phi) \\
O_4 &= \text{Tr}(\chi^\dagger \chi), O_5 = \text{Tr}(\chi^\dagger \tilde{\chi} + \tilde{\chi}^\dagger \chi).
\end{aligned} \quad (7)$$

Due to the  $C$  and  $CP$  symmetries,  $\mathcal{V}_0$  only involves combinations of  $(S+S^*)$  and  $SS^*$ . The interactions containing odd powers of  $(S-S^*)$  are forbidden as they are  $P$ -even but  $C$ -odd. Furthermore,  $(S-S^*)$  cannot mix with the Higgs multiplets in  $O_i$  because the five independent gauge-invariant combinations  $O_i (i=1, \dots, 5)$  in Eq. (7) are both  $P$ - and  $C$ -even. Other possible Higgs multiplet combinations such as  $\text{Tr}(\phi^\dagger \tilde{\phi} - \tilde{\phi}^\dagger \phi)$  and  $\text{Tr}(\Delta_L^\dagger \Delta_L - \Delta_R^\dagger \Delta_R)$  are  $P$ -odd, thus cannot couple to  $(S-S^*)$ . The terms proportional to even powers of  $(S-S^*)$  can be rewritten in terms of  $(S+S^*)^2$  and  $SS^*$ . The absence of odd power term of  $(S-S^*)$  means that  $S_D = (S-S^*)/(i\sqrt{2})$  is a potential DM candidate.

The spontaneous symmetry breaking (SSB) scheme is to realize the breaking pattern  $SU(2)_L \otimes SU(2)_R \otimes U(1)_{B-L} \rightarrow SU(2)_L \otimes U(1)_Y \rightarrow U(1)_{\text{em}}$ . After the SSB, the Higgs multiplets obtain nonzero VEVs

$$\langle \delta_{L,R}^0 \rangle = \frac{v_{L,R}}{\sqrt{2}}, \quad \langle \phi_{1,2}^0 \rangle = \frac{\kappa_{1,2}}{\sqrt{2}} \quad \text{and} \quad \langle \chi_{1,2}^0 \rangle = \frac{\xi_{1,2}}{\sqrt{2}}, \quad (8)$$

where  $\kappa_{1,2}$ ,  $\xi_{1,2}$ ,  $v_L$  and  $v_R$  are in general complex, and  $\kappa \equiv \sqrt{|\kappa_1|^2 + |\kappa_2|^2 + |\xi_1|^2 + |\xi_2|^2} \approx 246$  GeV represents the electroweak symmetry breaking scale. The value of  $v_R$  sets the scale of LR symmetry breaking which is directly linked to the right-handed gauge boson masses  $M_{W_R} = gv_R/\sqrt{2}$ . It is required that  $S_D$  does not develop a VEV directly from  $\mathcal{V}_0$ , namely  $CP$  is not broken by the singlet sector. It follows that after the SSB, although  $P$  and  $CP$  are both broken, there is a residual  $Z_2$  type of discrete symmetry on  $S_D$  in the gauge singlet sector, which is induced from the original  $CP$  symmetry.

Constraints on the parameter space from the DM relic density has been discussed in Ref. [15]. The main DM annihilation channels are  $S_D S_D \rightarrow W^\pm W^\mp, t\bar{t}$  and SM-like Higgs boson  $h^0 h^0$ . Making use of the constrained parameter space, we predicted the weakly interacting massive particle-nucleus elastic scattering cross section. The results show that the typical scattering cross section is about one order of magnitude below the current experimental upper bound. But in the enhanced Yukawa coupling case, the resulting spin-independent cross section can reach  $10^{-44} \text{cm}^2$  which is close to the improved bound set by the recent CDMS-II experiment [18].

The tiny soft  $C$ -breaking terms in  $\mathcal{V}_1$  may lead to the DM particle decay. The most general  $P$ -even but  $C$ -odd terms with dimension less than four are given by

$$-\mathcal{V}_1 = \mu_\epsilon (S - S^*) \left[ \sum_{i=1}^5 \zeta_i O_i + \zeta_6 (S + S^*)^2 + \zeta_7 (S - S^*)^2 \right]. \quad (9)$$

In this case, the  $S_D$  may decay dominantly into two lighter scalars such as  $\delta_L \delta_L$ . The lifetime of  $S_D$  is estimated by  $1/\tau_D \approx \mu_\epsilon^2 \sqrt{1 - 4m^2/m_D^2}/(16\pi m_D)$  for  $m \ll m_D$ , where  $m_D$  and  $m$  stand for the mass of  $S_D$  and final state scalars respectively. In order to have a lifetime around  $\mathcal{O}(10^{26} \text{s})$ , the required value of  $\mu_\epsilon$  is around  $10^{-23}$  GeV.

In this work we focus on the case in which  $\zeta_1 \gg \zeta_i$  ( $i = 2, \dots, 7$ ) and the right-handed triplet  $\Delta_R$  is much heavier than that of  $S_D$ , such that  $S_D$  will decay dominantly into left-handed triplet  $\Delta_L$  as shown in Fig. 1.

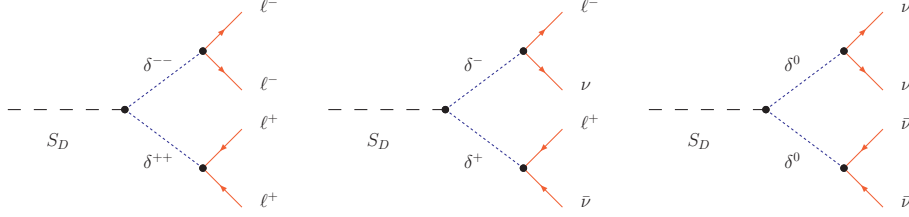


FIG. 1: Feynman diagrams for DM particle  $S_D$  decaying into charged leptons and neutrinos through intermediate  $SU(2)_L$  triplets  $\delta_L^{++}\delta_L^{--}$ ,  $\delta_L^+\delta_L^-$  and  $\delta_L^0\delta_L^0$ .

The triplets with non-zero lepton number do not couple to quarks directly. The Yukawa interaction between the scalars and leptons is

$$\begin{aligned} \mathcal{L}_Y = & -\bar{\ell}_{Li}(h_{ij}\phi + \tilde{h}_{ij}\tilde{\phi} + g_{ij}\chi + \tilde{g}_{ij}\tilde{\chi})\ell_{Rj} \\ & - y_{ij}(\bar{\ell}_{Li}^c i\tau_2 \Delta_L \ell_{Lj} + \bar{\ell}_{Ri}^c i\tau_2 \Delta_R \ell_{Rj}) + h.c., \end{aligned} \quad (10)$$

which leads to the following seesaw formula for left-handed neutrino mass matrix

$$M_\nu = M_L - M_D \frac{1}{M_R} M_D^T \quad (11)$$

with  $(M_{L(R)})_{ij} = y_{ij}v_{L(R)}/\sqrt{2}$  and  $(M_D)_{ij} = (h_{ij}\kappa_1 + \tilde{h}_{ij}\kappa_2^* + g_{ij}\xi_1 + \tilde{g}_{ij}\xi_2^*)/\sqrt{2}$ . The upper bound for  $v_L$  from neutrino masses is around a few eV, and that from the  $\rho$ -parameter in electroweak precision measurements is about 1 GeV. The absence of  $W_R$  from collider searches sets a lower bound of  $v_R \gtrsim \mathcal{O}(\text{TeV})$ . Thus the hierarchies in neutrino masses, SM gauge boson masses and the right-handed gauge boson masses require that

$$v_L \ll \kappa \ll v_R. \quad (12)$$

An important consequence of the smallness of  $v_L$  is that the couplings between left-handed triplets and SM gauge bosons  $W^\pm$  and  $Z^0$  are strongly suppressed, as  $\delta_L^{\pm\pm}W^\mp W^\mp$ ,  $\delta_L^\pm W^\mp Z^0$  and  $\delta_L^0 Z^0 Z^0$  couplings are all proportional to  $v_L$ . For instance, the ratio between the decay width of  $\delta_L^{++} \rightarrow \ell^+\ell^+$  and  $\delta_L^{++} \rightarrow W^+W^+$  is given by

$$\frac{\Gamma(\delta_L^{++} \rightarrow W^+W^+)}{\Gamma(\delta_L^{++} \rightarrow \ell^+\ell^+)} \approx \frac{g^4}{16} \left( \frac{v_L m_{\delta_L}}{Y_{\ell\ell} m_W^2} \right)^2, \quad (13)$$

where  $Y_{\ell\ell}$  is the Yukawa coupling between  $\delta_L^{++}$  and charged lepton  $\ell^+$ . For the typical case  $v_L \sim \mathcal{O}(10^{-9})$  GeV and  $m_{\delta_L} \sim \mathcal{O}(10^3)$  GeV,  $\Gamma(\delta_L^{++} \rightarrow \ell^+\ell^+)$  is always dominant over  $\Gamma(\delta_L^{++} \rightarrow W^+W^+)$  as long as the Yukawa coupling is not too small, namely,  $Y_{\ell\ell} \gtrsim 10^{-10}$ .

Similar results are found for the  $W^\pm Z^0$ ,  $Z^0 Z^0$  and  $h^0 h^0$  final states. Thus a small  $v_L$  required by the tiny neutrino masses naturally suppresses the triplet non-leptonic decays channels, such that our model can avoid the constraints from the PAMELA anti-proton data.

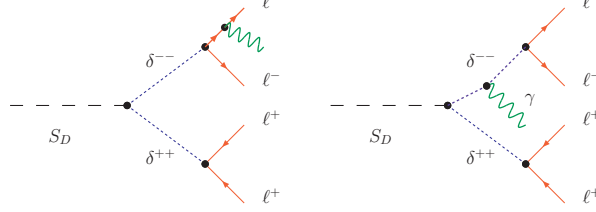


FIG. 2: Feynman diagrams for gamma-ray emission through internal bremsstrahlung. (Left) final state radiation (FSR) from final state charged leptons. (Right) virtual internal bremsstrahlung (VIB) from doubly charged triplet scalars.

The Yukawa interaction term  $\bar{\ell}_L^c i \tau_2 \Delta_L \ell_L$  requires that the couplings  $\delta_L^{\pm\pm} l^\mp l^\mp$ ,  $\delta_L^0 \nu \nu$  and  $\delta_L^{\pm} l^\mp \nu$  are the same within each generation in the flavor basis. If the positron excesses reported by the PAMELA and Fermi-LAT are indeed from the DM decay through triplets, there must exist associating high energy neutrino flux which can be detected by the future experiments.

The  $SU(2)$  triplet contains doubly as well as singly charged scalars. Besides the ordinary ICS and FSR caused by the final state charged leptons, the charged triplet scalars will emit gamma-rays through VIB processes in the cascade decay  $S_D \rightarrow \delta_L^{\pm\pm} \delta_L^{\mp\mp} \gamma$  as shown in Fig. 2. The photon multiplicity for a decay process  $S \rightarrow XX$  is defined as [19]

$$\frac{dN_{XX}}{dx} \equiv \frac{1}{\sigma_{S \rightarrow XX}} \frac{d\sigma_{S \rightarrow XX\gamma}}{dx}, \quad (14)$$

where  $x = 2E_\gamma/\sqrt{s}$  and  $\sqrt{s} = m_S$  is the center-of-mass energy. The radiation is dominated by the collinear photon emission case, which can be approximated by

$$\frac{dN_{XX}}{dx} \approx \frac{\alpha Q^2}{\pi} F(x) \log \left( \frac{s(1-x)}{m_X^2} \right) \quad (15)$$

with  $F(x) = (1 + (1-x)^2)/x$  for fermions and  $(1-x)/x$  for bosons. For the decay process  $S_D \rightarrow \delta_L^{\pm\pm} \delta_L^{\mp\mp}$ , one has  $s = m_D^2$  and  $m_X = m_{\delta_L}$ . For the sequential decay  $\delta_L^{\pm\pm} \rightarrow \ell^\pm \ell^\pm$ ,  $s$  and  $m_X$  are replaced by  $m_{\delta_L}$  and  $m_\ell$  respectively. For doubly charged particles there is a factor of four enhancement relative to that of singly charged ones. The final positron and gamma-ray energy spectra of cascade decays, such as  $S_D \rightarrow \delta_L^{\pm\pm} \delta_L^{\mp\mp} \rightarrow 4\ell$ , depend on the



mass of the intermediate states, which also provide a possibility to probe the masses of the triplets.

### III. ENERGY SPECTRA OF THE COSMIC-RAY PARTICLES

The dark matter cascade decay processes  $S_D \rightarrow \delta_L \delta_L \rightarrow 4\ell$ ,  $2\ell 2\nu$  and  $4\nu_\ell$  contribute to new sources of primary positrons, neutrinos and gamma-rays in our galaxy. Besides the mass and lifetime of  $S_D$ , the final energy spectra of the cosmic-ray particles depend on the mass ratio between  $S_D$  and the triplets. In this section, we consider two typical mass hierarchies: the small mass hierarchy case **(SH)**, in which we take the mass ratio  $r_m \equiv 2m_{\delta_L}/m_D = 0.8$ , and the large hierarchy case **(LH)** in which  $r_m = 0.1$ . Note that in the two extreme cases with  $r_m = 1$  and 0, the shape of the final energy spectra should reduce to that of the two-body and four-body decays respectively. The relative strengths of the Yukawa couplings also play important roles, as they determine the corresponding branching ratios of different decay modes. In the basis in which the left-handed weak gauge interaction is diagonal, the leptonic Yukawa couplings  $Y_{ij}$  ( $i, j = e, \mu, \tau$ ) are related to  $y_{ij}$  by  $Y = U^T \cdot y \cdot U$ , where  $U$  is the mixing matrix for charged lepton. For the Yukawa couplings, we are going to consider four representative cases. In each of the first three cases, the Yukawa couplings are assumed to be dominant by one of the three generation leptons, while in the last case the couplings are assumed to be the same for all the generations, i.e., **I**)  $|Y_{ee}| \gg |Y_{\mu\mu}|, |Y_{\tau\tau}|$ , the triplet scalars decay mainly into  $4e$ ,  $2e2\nu_e$  and  $4\nu_e$ ; **II**)  $|Y_{\mu\mu}| \gg |Y_{ee}|, |Y_{\tau\tau}|$ , the triplets decay mainly into  $4\mu$ ,  $2\mu 2\nu_\mu$  and  $4\nu_\mu$ ; **III**)  $|Y_{\tau\tau}| \gg |Y_{ee}|, |Y_{\mu\mu}|$ , the triplets decay mainly into  $4\tau$ ,  $2\tau 2\nu_\tau$  and  $4\nu_\tau$ ; and **IV**)  $|Y_{ee}| \approx |Y_{\mu\mu}| \approx |Y_{\tau\tau}|$ , the triplet scalars decay to all leptons with the same branching ratio. In fact, the case IV will give the same results for the flavor democratic case in which all the Yukawa matrix elements are nearly identical. For simplicity we have assumed that the off-diagonal Yukawa couplings  $Y_{ij}$  ( $i \neq j$ ) are all small such that no lepton flavor violating process are considered. For each case, we consider various values of the mass and lifetime of  $S_D$  with paying attention to the case that can reproduce the current data. Note that in this model, the large mass hierarchy  $r_m = 0.1$  is unlikely for the cases LH-I and LH-II unless  $S_D$  is much heavier than 10 TeV, since the lower bounds of the triplet masses are expected to be around TeV scale. However, we still keep them for the sake of completeness as such light intermediate states may be possible in other models.

### A. Electrons and positrons

In the Milky Way, the propagation of cosmic-ray (CR) particles can be approximated by a two-zone propagation model, which includes two cylinders centered at the galactic center. A cylinder of radius  $R = 20$  kpc with height  $2L$  ( $L = 1 - 20$  kpc) in the  $z$  direction delimits the CR propagation region. A smaller cylinder with the same radius but with thickness  $2h_z = 0.2$  kpc models the galactic plane. The solar system is located at  $r_\odot = 8.5$  kpc and  $z_\odot = 0$ . In general, the CR propagation equations contain terms for convection and reacceleration effects [20]. However, for electrons and positrons with energy  $E \gtrsim 10$  GeV, these effects can safely be neglected [21]. Thus one only needs to consider the diffusion effect. In this case, the steady-state diffusion equation for positron is given by

$$-K(E) \cdot \nabla^2 f_{e^+} - \frac{\partial}{\partial E}(b(E)f_{e^+}) = Q, \quad (16)$$

where  $f_{e^+}(E, r, z)$  is the positron differential number density in cylinder coordinate and  $K(E) = K_0(E/\text{GeV})^\delta$  is the spatial diffusion coefficient. Through fitting the measured ratio of boron to carbon (B/C), the propagation parameters  $\delta$ ,  $K_0$  and  $L$  can be determined [22]. In Table. I, we list three typical combinations of the propagation parameters [21, 23]. The parameter set MIN and MAX corresponds to the minimal and maximal positron flux respectively, while the MED scenario best fits the B/C ratio and produce the moderate flux. The energy loss rate  $b(E)$  are mainly due to the ICS and synchrotron processes. The two processes combined give  $b(E) = E^2/(\text{GeV} \cdot \tau_E)$  with  $\tau_E = 10^{16}$  s [24]. For decaying DM model, the source term  $Q$  is given by

$$Q(r, E) = \frac{\rho(r)}{m_D} \sum_k \Gamma_k \frac{dn_{e^+}^k}{dE}, \quad (17)$$

where  $\Gamma_k$  is the decay width and  $k$  runs over all the channels with positrons in the final states.  $dn_{e^+}^k/dE$  is the positron energy spectrum per DM decay. The DM halo profile  $\rho(r)$  is usually parameterized as a spherically symmetric form

$$\rho(r) = \rho_\odot \left(\frac{r_\odot}{r}\right)^\gamma \left(\frac{1 + (r_\odot/r_s)^\alpha}{1 + (r/r_s)^\alpha}\right)^{(\beta-\gamma)/\alpha} \quad (18)$$

with local DM density  $\rho_\odot = 0.3 \text{ GeV cm}^{-3}$ . Possible DM halo profile parameters  $\alpha, \beta, \gamma$  and  $r_s$  are listed in Table. II. In this paper, we adopt the NFW profile and MED propagation model in numerical calculations.

Propagation	$\delta$	$K_0$ (kpc <sup>2</sup> /Myr)	$L$ (kpc)
MED	0.70	0.0112	4
MAX	0.46	0.0765	15
MIN	0.55	0.00595	1

TABLE I: Three typical combinations for the propagation parameters  $\delta$ ,  $K_0$  and  $L$  from the measured B/C ratio [21, 23].

Halo Profile	$\alpha$	$\beta$	$\gamma$	$r_s$ (kpc)
NFW	1	3	1	20
Isothermal	2	2	0	5
Moore	1.5	3	1.3	30

TABLE II: The values of parameters  $\alpha, \beta, \gamma$  and  $r_s$  for the NFW [25], Isothermal [26] and Moore [27] DM halo profiles.

Eq. (16) can be solved analytically from the above considerations. For the decaying dark matter, the solution of the positron diffusion can be written as [23, 28]

$$f_{e^+}(E, r, z) = \frac{1}{m_D} \int_E^{m_D} dE' G_{e^+}(E, E', r, z) \sum_k \Gamma_k \frac{dn_{e^+}^k}{dE'} , \quad (19)$$

The explicit form of the Green's function  $G_{e^+}(E, E', r, z)$  is given by

$$G_{e^+}(E, E', r, z) = \sum_{n,m=1}^{\infty} G_{nm} \frac{\tau_E}{E^2} J_0 \left( \zeta_n \frac{r}{R} \right) \sin \left[ \frac{m\pi}{2L} (z - L) \right] \\ \times \exp \left[ K_0 \tau_E \left( \frac{\zeta_n^2}{R^2} + \frac{m^2 \pi^2}{4L^2} \right) \left( \frac{E^{\delta-1} - E'^{\delta-1}}{\delta - 1} \right) \right] , \quad (20)$$

with

$$G_{nm} = \frac{2}{J_1^2(\zeta_n) R^2 L} \int_0^R dr' r' J_0 \left( \zeta_n \frac{r'}{R} \right) \int_{-L}^L dz' \rho(r', z') \sin \left[ \frac{m\pi}{2L} (z' - L) \right] , \quad (21)$$

where  $J_{0(1)}$  is the zeroth(first)-order Bessel function.  $\zeta_n$  are successive zeros of the function  $J_0$ . At the heliosphere boundary ( $r = r_\odot$  and  $z = 0$ ), the interstellar positron flux per unit energy from the DM decay is

$$\Phi_{e^+}^{DM}(E) = \frac{c}{4\pi} f_{e^+}(E, r_\odot, 0) . \quad (22)$$

The interstellar  $e^-$  and  $e^+$  background is approximated by [24]

$$\begin{aligned}\Phi_{e^-}^{prim}(E) &= \frac{0.16E^{-1.1}}{1 + 11E^{0.9} + 3.2E^{2.15}} , \\ \Phi_{e^-}^{sec}(E) &= \frac{0.7E^{0.7}}{1 + 110E^{1.5} + 600E^{2.9} + 580E^{4.2}} , \\ \Phi_{e^+}^{sec}(E) &= \frac{4.5E^{0.7}}{1 + 650E^{2.3} + 1500E^{4.2}} ,\end{aligned}\tag{23}$$

where  $E$  and  $\Phi$  are in units of GeV and  $\text{GeV}^{-1}\text{cm}^{-2}\text{s}^{-1}\text{sr}^{-1}$ , respectively. The interstellar (IS) positron fraction is given by

$$PF(E_{IS}) = \frac{\Phi_{e^+}^{DM} + k_+ \Phi_{e^+}^{sec}}{\Phi_{e^+}^{DM} + \Phi_{e^-}^{DM} + k_+ \Phi_{e^+}^{sec} + k_- (\Phi_{e^-}^{prim} + \Phi_{e^-}^{sec})} .\tag{24}$$

where we have introduced two real parameters  $k_+$  and  $k_-$  to normalize the positron and electron background, which reflects the background uncertainties [29]. In the numerical calculations we take  $k_+(k_-) = 0.9(0.7)$ .

For the solar modulation effects we adopt the Gleeson and Axford analytical force-field approximation in which the final flux  $\Phi(E_\oplus)$  at the top of atmosphere is given by

$$\Phi(E_\oplus) = \frac{p_\oplus^2}{p_{IS}^2} \Phi(E_{IS}) ,\tag{25}$$

where  $\Phi(E_{IS})$  denotes the primordial interstellar flux.  $E_{IS}$  and  $E_\oplus$  have the following relation

$$E_{IS} = E_\oplus + |Ze|\phi_F ,\tag{26}$$

where  $|Z| = 1$  is the  $e^\pm$  charge number. For the solar modulation parameter  $\phi_F$ , we take a typical value of  $\phi_F = 500$  MV. We assume that the solar modulation effect is the same for electron and positron, which leads to  $PF(E_\oplus) = PF(E_{IS})$ . Note that even in the case of charge-independent modulation, the solar modulation effect leads to a translation for the positron factor  $PF$ , thus must be considered.

Making use of the above mentioned formulas we calculate the positron fraction and the total electron and positron flux for the eight cases SH(LH)-I~IV. The injection spectra  $dn_e^k/dE$  is obtained by using the package Pythia 8.1 [30]. In each case we consider some typical values of the parameters  $m_D$  and  $\tau_D$  which can reproduce the experimental data well. The favored values for the parameters are listed in Tab. III and the corresponding numerical results are given in Fig. 3. From the case SH(LH)-I to SH(LH)-III, the required mass of  $S_D$  increases from 2 to 8 TeV while the lifetime decreases from  $\tau_D = 1.5 \times 10^{26}$  s to

case	$m_D$ (TeV)	$\tau_D$ ( $10^{26}$ s)	$2m_{\delta_L}/m_D$
SH(LH)-I	2.0	1.5	0.8 (0.1)
SH(LH)-II	4.0	0.9	0.8 (0.1)
SH(LH)-III	8.0	0.4	0.8 (0.1)
SH(LH)-IV	2.5	1.3	0.8 (0.1)

TABLE III: Typical values of the mass and lifetime of  $S_D$  as well as  $m_{\delta_L}$  favored by the PAMELA and Fermi-LAT (or ATIC) data in different cases from SH(LH)-I to SH(LH)-IV.

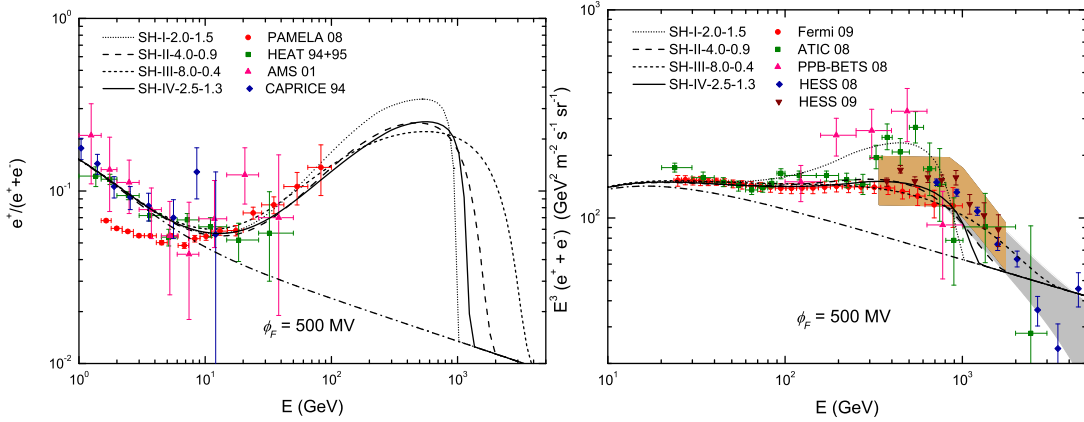


FIG. 3: The predicted positron fraction (left) and the total electron and positron flux (right) for four representative cases from SH-I to SH-IV. The relevant parameters are given in the figures in compact notations. For instance, the notation "SH-II-4.0-0.9" corresponds to the case of SH-II with  $m_D=4.0$  TeV and  $\tau_D = 0.9 \times 10^{26}$ s.

$\tau_D = 0.4 \times 10^{26}$  s. The case SH(LH) -IV is a kind of mixture with equal Yukawa couplings for all generation leptons, and the required mass and lifetime are found close to the case SH(LH)-I. As indicated in Fig. 3, the SH-I case can explain both the PAMELA and ATIC data. In this case, the DM particle decays directly into  $4e$ , which usually leads to a too hard spectrum to meet the Fermi-LAT data. The SH-II~IV cases involving  $\mu$ - and  $\tau$ -lepton as final states can reproduce the PAMELA and Fermi-LAT results well with the parameters in Tab. III. The differences among the four cases are not obvious in the low energy range  $E \lesssim 100$  GeV. However, in higher energy range  $E \gtrsim 1$  TeV, the heavier final state case leads to harder energy spectrum. The SH-III case with  $4\tau$  final states has the hardest spectrum among all the cases in this energy region.

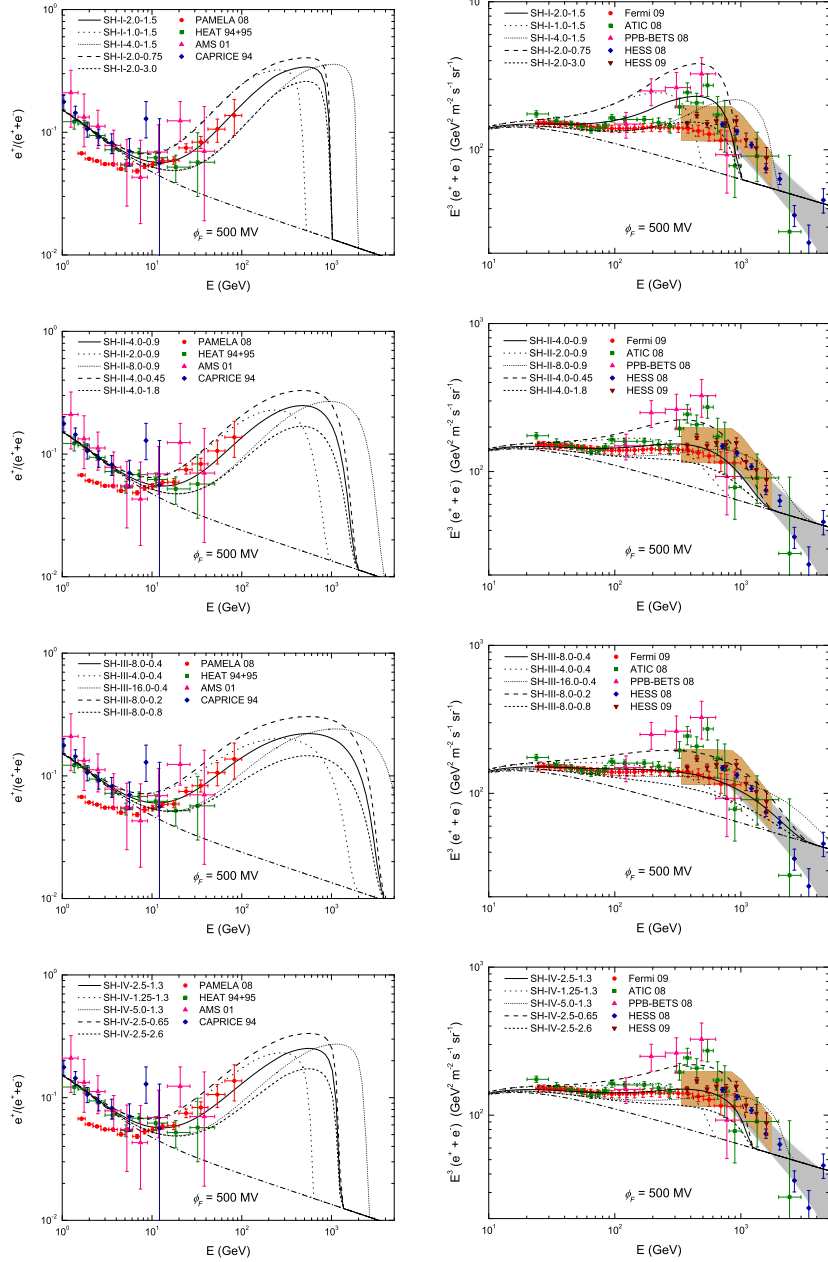


FIG. 4: Effects of the DM particle mass and lifetime on the positron fraction (left) and the total electron and positron flux (right) for four representative cases from SH-I to SH-IV. For each case the mass and life-time of  $S_D$  are varied by a factor of two.

The mass and lifetime of  $S_D$  are two key parameters in determining the positron fraction and the total electron and positron flux. In Fig. 4, we vary the DM mass or lifetime by a factor of two for each case listed in Tab. III. The results show that in general the location of the peak in the spectrum is controlled by  $m_D$ , and the height of the peak is more relevant to

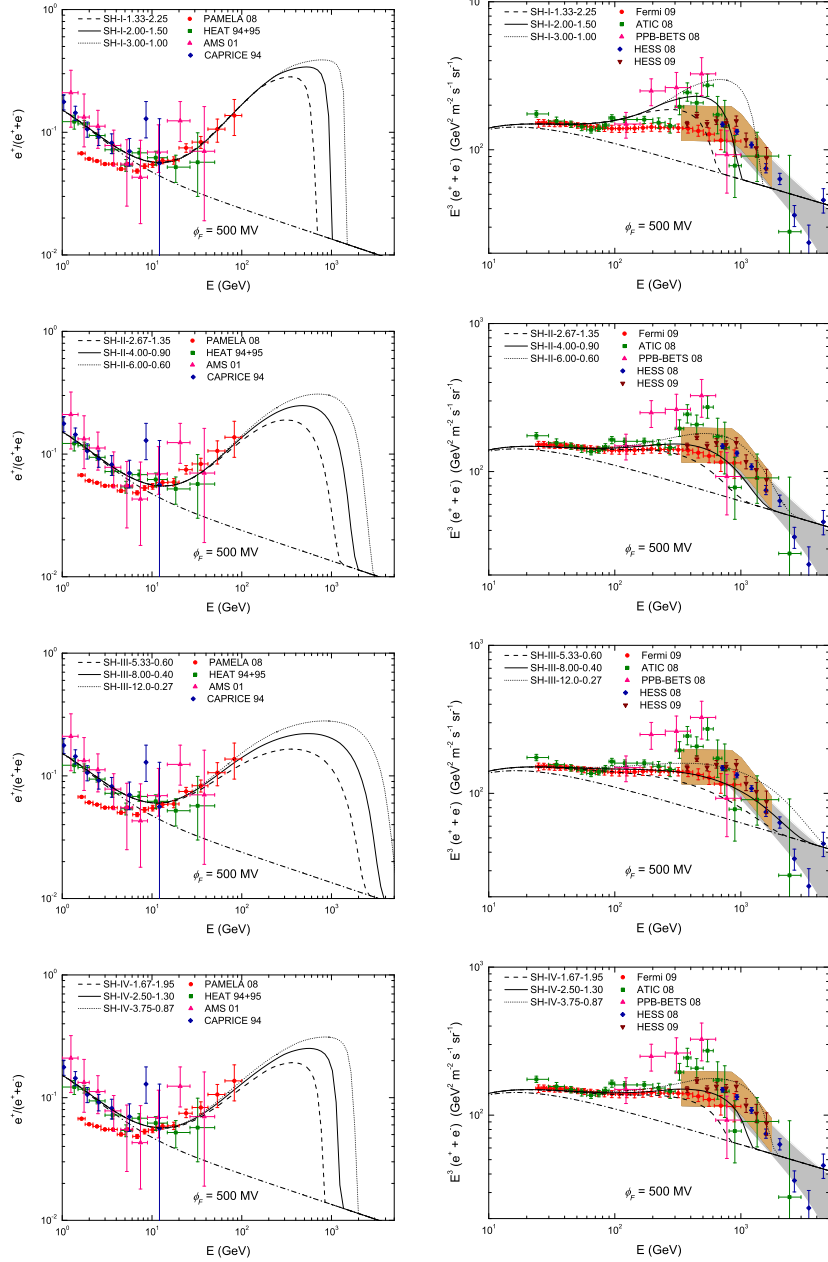


FIG. 5: The same as Fig. 4, but for different mass and lifetime of  $S_D$  which can have nearly the same results for the positron fraction but significantly differ in the total flux of electron and positron. See text for detailed explanation.

$\tau_D$ . Compared with the PAMELA data, the Fermi-LAT data is more sensitive to  $m_D$ , which is due to more data points at high energy region and higher statistics. If simultaneously adjusting both  $m_D$  and  $\tau_D$ , in all the cases from SH-I to SH-IV, one can obtain the nearly the same positron fraction ( $E \lesssim 100$  GeV) to explain the PAMELA data as shown in Fig.

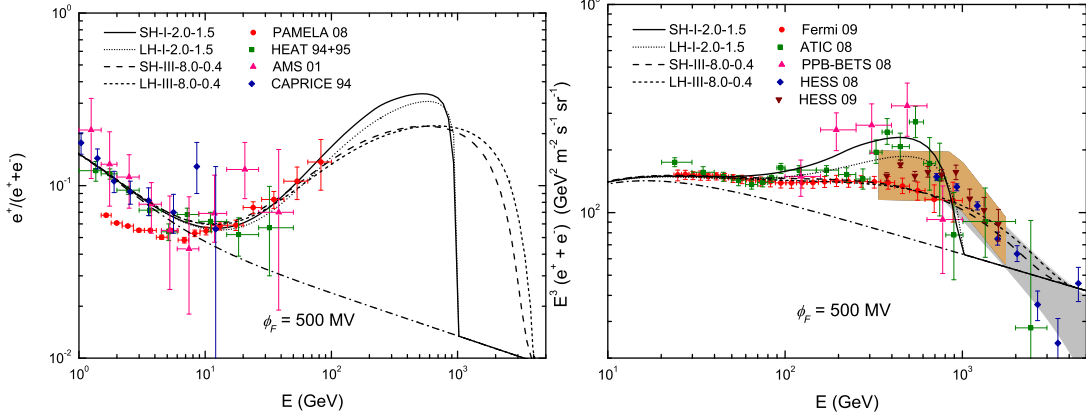


FIG. 6: Difference between the small and large hierarchy scenarios in the positron fraction (left) and the total flux of electron and positron (right) for the cases SH(LH)-I and SH(LH)-II.

5. However, the predicted total electron and positron flux are obvious different.

For a comparison between SH and LH cases, we show in Fig. 6 the results for SH(LH)-I and SH(LH)-III. It is clear that the differences are rather mild for the parameters given in Tab. III. Actually, the SH and LH cases have significant differences in the injection energy spectrum  $dn_{e^+}^k/dE$ . However, the differences are smeared out due to the energy loss processes from the ICS and the synchrotron.

## B. Neutrinos

The expected muon neutrino flux coming from the galactic center (GC) and arriving at the Earth can be estimated by [31]

$$\frac{d\Phi_{\nu_\mu}}{dE_{\nu_\mu}} = \rho_\odot r_\odot \frac{1}{4\pi m_D} \left( \sum_{\alpha=e,\mu,\tau} P_{\nu_\alpha \rightarrow \nu_\mu} \sum_k \Gamma_k \frac{dn_{\nu_\alpha}^k}{dE_{\nu_\alpha}} \right) J_{\Delta\Omega} \Delta\Omega, \quad (27)$$

where the neutrino oscillation probabilities  $P_{\nu_\alpha \rightarrow \nu_\mu}$  are  $P_{\nu_e \rightarrow \nu_\mu} = 0.22$ ,  $P_{\nu_\mu \rightarrow \nu_\mu} = 0.39$  and  $P_{\nu_\tau \rightarrow \nu_\mu} = 0.39$  [32]. One can have the same results for the muon anti-neutrino flux  $\Phi_{\bar{\nu}_\mu}$ . The averaged number flux  $J_{\Delta\Omega}$  in a cone with half-angle  $\phi$  around GC is given by

$$J_{\Delta\Omega} = \frac{1}{\rho_\odot r_\odot} \frac{1}{\Delta\Omega} \int_{\Delta\Omega} d\Omega \int_{LOS} \rho(l) dl, \quad (28)$$

where  $\Delta\Omega = 2\pi(1 - \cos\phi)$  is the solid angle. The above equation can be written as the following form

$$J_{\Delta\Omega} = \frac{1}{\rho_\odot r_\odot} \frac{2\pi}{\Delta\Omega} \int_{\cos\phi}^1 d\cos\phi' \int_0^{l_{max}} \rho \left( \sqrt{r_\odot^2 - 2lr_\odot \cos\phi' + l^2} \right) dl, \quad (29)$$



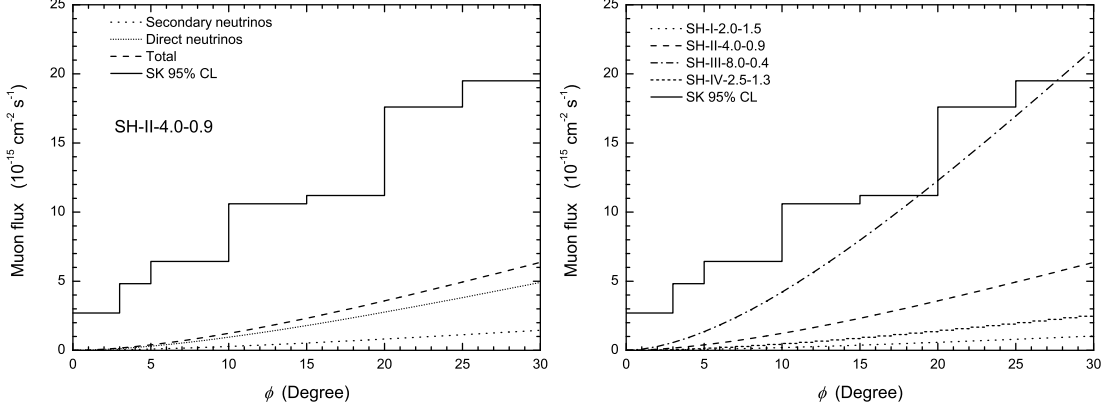


FIG. 7: The predicted neutrino-induced upgoing muon flux as a function of the cone half-angle around the galactic center. (left) the direct and secondary neutrino contributions in the SH-II case. (Right) the predicted total neutrino-induced upgoing muon flux for the cases SH-I  $\sim$  SH-IV.

where the integration upper limit  $l_{max} = \sqrt{r_{MW}^2 - r_{\odot}^2 \sin^2 \phi'} + r_{\odot} \cos \phi'$  and the DM halo size  $r_{MW} \approx 30$  kpc.

The muon neutrinos interact with the earth rock to produce the upgoing muon flux, which can be detected by the water Cherenkov detector Super-Kamiokande (SK) [33, 34]. The neutrino induced muon flux is give by [35]

$$\Phi_{\mu} = \int_{E_{thr}}^{m_D/2} dE_{\nu_{\mu}} \frac{d\Phi_{\nu_{\mu}}}{dE_{\nu_{\mu}}} \int_{E_{thr}}^{E_{\nu_{\mu}}} dE_{\mu} L(E_{\mu}) \sum_{a=p,n} n_a \sum_{x=\nu_{\mu}, \bar{\nu}_{\mu}} \frac{d\sigma_x^a(E_{\nu_{\mu}})}{dE_{\mu}}. \quad (30)$$

where  $L(E_{\mu})$  is the range of a muon with energy  $E_{\mu}$  until its energy drops below the SK threshold  $E_{thr} = 1.6$  GeV:

$$L(E_{\mu}) = \frac{1}{\rho \beta_{\mu}} \ln \frac{\alpha_{\mu} + \beta_{\mu} E_{\mu}}{\alpha_{\mu} + \beta_{\mu} E_{thr}}, \quad (31)$$

where  $\alpha_{\mu} = 2 \times 10^{-3} \text{ g}^{-1} \text{ GeV cm}^2$  and  $\beta_{\mu} = 4.2 \times 10^{-6} \text{ g}^{-1} \text{ cm}^2$ .  $\rho$  is the density of the material in  $\text{g cm}^{-3}$  and  $n_a \approx r_a \rho / m_p$  are the number densities of neutrons and protons with  $r_p \approx 5/9$  and  $r_n \approx 4/9$ . For the detection cross section, we use

$$\frac{d\sigma_x^a(E_{\nu_{\mu}})}{dE_{\mu}} \approx \frac{2m_p G_F^2}{\pi} \left( A_x^a + B_x^a \frac{E_{\mu}^2}{E_{\nu_{\mu}}^2} \right), \quad (32)$$

where  $A_{\nu_{\mu}}^{n,p} = 0.25, 0.15$ ,  $B_{\nu_{\mu}}^{n,p} = 0.06, 0.04$  and  $A_{\bar{\nu}_{\mu}}^{n,p} = B_{\nu_{\mu}}^{p,n}$ ,  $B_{\bar{\nu}_{\mu}}^{n,p} = A_{\nu_{\mu}}^{p,n}$ .

As mentioned in Sec II, an important feature of this model is that the Yukawa couplings for  $\delta_L^{++} \ell^- \ell^-$ ,  $\delta_L^{+} \ell^- \nu_{\ell}$  and  $\delta_L^0 \nu_{\ell} \nu_{\ell}$  are equal. In the DM particle decay processes, the final state

neutrinos may come from the direct decay of  $\delta_L$  and from the secondary decay of charged leptons. If a large decay rate of  $\delta_L^{++} \rightarrow \ell^+ \ell^+$  is needed for explaining the current experimental data, the associated processes  $\delta_L^+ \rightarrow \ell^+ \nu_\ell$  and  $\delta_L^0 \rightarrow \nu_\ell \nu_\ell$  will give extra contributions to the neutrino flux, which can be more important than that neutrinos from the secondary decay of charged leptons. In Fig. 7, we compare the contributions to the total neutrino-induced muon flux from the direct neutrinos and that from the secondary lepton decays in the SH-II case. The difference can be clearly seen in the large angle region  $\phi \simeq 30^\circ$  in which the direct neutrino contribution is roughly five times as many as that from secondary charged lepton decays. In Fig. 7, we also give the predicted muon flux for the cases SH-I  $\sim$  SH-IV. The results show that the SH-III case with  $S_D$  decaying into  $4\tau, 2\tau 2\nu_\tau$  and  $4\nu_\tau$  predicts much larger flux than the other cases. The reason is that the direct neutrinos in this case have higher energy than that in other cases. This case can be tested in the future experiments with improved sensitivity by a factor of a few. Note that the  $2\tau$  or  $4\tau$  final state cases are now strongly disfavored by the latest Fermi-LAT gamma-ray data [36] even in the DM decay scenario. The predictions for the cases LH-I  $\sim$  LH-IV are found to be very similar.

### C. Gamma-rays

The high energy gamma-rays generated by DM particle may come from two type of contributions. The first one is that the DM particle directly produces high energy gamma-rays through processes VIB and FSR. The second contribution comes from the ICS process. In this case, the low energy interstellar photons obtain energy from the high energy positrons and electrons. For the first contribution, the expected spectrum of high energy gamma-rays is given by

$$\frac{d\Phi_\gamma}{dE_\gamma} = \frac{\rho_\odot r_\odot}{4\pi m_D} J_{\Delta\Omega} \left( \sum_k \Gamma_k \frac{dn_\gamma^k}{dE_\gamma} \right), \quad (33)$$

where  $J_{\Delta\Omega}$  is defined in the same way as for neutrino in Eq. (28). For a general observable region, it is convenient to choose the galactic coordinate  $(b, l)$  where  $b$  and  $l$  stand for the galactic latitude and longitude. Then  $J_{\Delta\Omega}$  can be written as the following form

$$J_{\Delta\Omega} = \frac{1}{\rho_\odot r_\odot} \frac{1}{\Delta\Omega} \int_{\Delta\Omega} d\Omega \int_0^{s_{max}} \rho \left( \sqrt{r_\odot^2 - 2sr_\odot \cos b \cos l + s^2} \right) ds, \quad (34)$$

where the integration upper limit  $s_{max} = \sqrt{r_{MW}^2 - r_\odot^2(1 - \cos^2 b \cos^2 l)} + r_\odot \cos b \cos l$  and  $d\Omega = \cos b db dl$ .

The high energy gamma-rays produced by the ICS process  $e^\pm\gamma \rightarrow e^\pm\gamma'$  have the following energy spectrum [37, 38]:

$$\frac{d\Phi_{\gamma'}}{dE_{\gamma'}} = \frac{\alpha_{em}^2}{\Delta\Omega} \int_{\Delta\Omega} d\Omega \int_{LOS} ds \int \int f_{e^+}(E_e, r, z) u_\gamma(E_\gamma, r, z) f_{ICS} \frac{dE_e}{E_e^2} \frac{dE_\gamma}{E_\gamma^2} . \quad (35)$$

Since the photon may be emitted from both electron and positron, an overall factor of 2 has been multiplied in the equation. The differential energy density  $u_\gamma(E_\gamma, r, z)$  of interstellar radiation field (ISRF) contains three components: the cosmic microwave background (CMB), thermal dust radiation and star light. Here we adopt the GALPROP numerical result for  $u_\gamma$  in Ref. [39]. The parameter  $f_{ICS}$  is defined by [37]

$$f_{ICS} = 2q \ln q + (1 + 2q)(1 - q) + \frac{1}{2} \frac{\epsilon^2}{1 - \epsilon} (1 - q) , \quad (36)$$

with

$$\epsilon = \frac{E_{\gamma'}}{E_e}, \quad q = \frac{E_{\gamma'} m_e^2}{4E_\gamma E_e (E_e - E_{\gamma'})} , \quad (37)$$

where  $0 \leq q \leq 1$ . In Eq. (35),  $f_{e^+}(E_e, r, z)$  is the positron differential number density. Because of the ICS and synchrotron, high energy electrons and positrons will loss most of their energy within a kpc. Therefore one may neglect the diffusion term of Eq. (16) and approximately calculate  $f_{e^+}(E_e, r, z)$  for every point in the CR propagation region. In this case,  $f_{e^+}(E_e, r, z)$  is given by the following formulas [37, 40]

$$f_{e^+}(E_e, r, z) = \frac{1}{b_{ICS}(E_e, r, z)} \frac{\rho(r, z)}{m_D} \sum_k \Gamma_k \int_{E_e}^{m_D} dE' \frac{dn_{e^+}^k}{dE'} , \quad (38)$$

where the electron energy loss rate  $b_{ICS}(E_e, r, z)$  is

$$b_{ICS}(E_e, r, z) = \frac{2\pi\alpha_{em}^2}{E_e^2} \int dE_\gamma \frac{u_\gamma(E_\gamma, r, z)}{E_\gamma^2} \int dE_{\gamma'} (E_{\gamma'} - E_\gamma) f_{ICS} . \quad (39)$$

Here we neglect the synchrotron energy loss rate  $b_{syn}$  as  $b_{syn} \ll b_{ICS}$  [38]. It is worthwhile to stress that the above energy loss rate  $b_{ICS}(E_e, r, z)$  is position dependent<sup>1</sup>.

In order to compare with the experimental data, one needs to know the diffuse gamma-ray background which includes a galactic  $\Phi_\gamma^{\text{Galactic}}$  contribution and an extragalactic (EG)  $\Phi_\gamma^{\text{EG}}$  contribution. The galactic gamma-ray background  $\Phi_\gamma^{\text{Galactic}}$  mainly comes from pion

---

<sup>1</sup> If a position independent energy loss rate is assumed, one can use Eq. (19) to calculate  $f_{e^+}(E_e, r, z)$ .

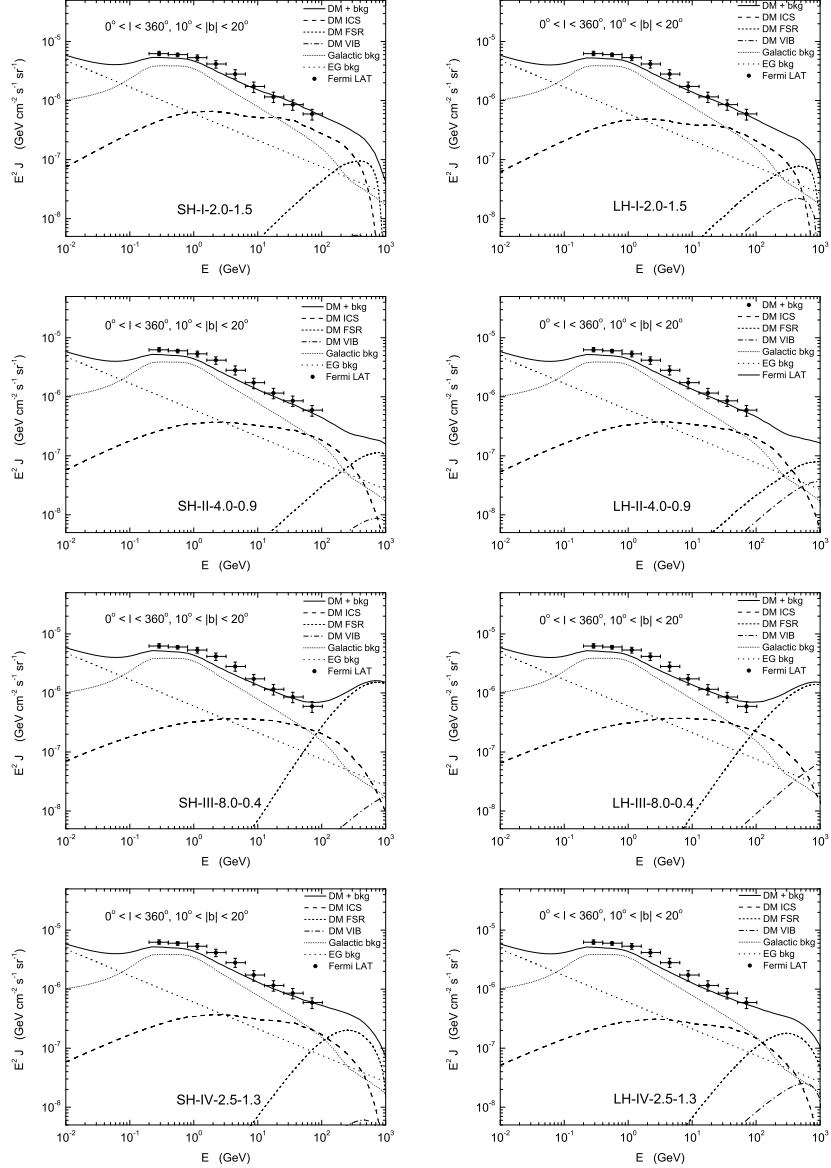


FIG. 8: The predicted gamma-ray spectra in the small hierarchy (left) and large hierarchy (right) scenarios for the observed region  $10^\circ < |b| < 20^\circ$ .

decay, ICS and bremsstrahlung. In principle, one should run the GALPROP code [20] to obtain  $\Phi_\gamma^{\text{Galactic}}$  for given diffusion parameters  $\delta$ ,  $K_0$  and  $L$ . Note that  $\Phi_\gamma^{\text{Galactic}}$  is not sensitive to these given diffusion parameters as shown in Refs. [41]. For an illustration, we use the numerical results of the conventional GALPROP model (44.500180) in Ref. [42] as an estimate of our galactic gamma-ray background  $\Phi_\gamma^{\text{Galactic}}$ . For the diffuse extragalactic gamma-ray background, one can adopt the following parametrization from the Fermi-LAT

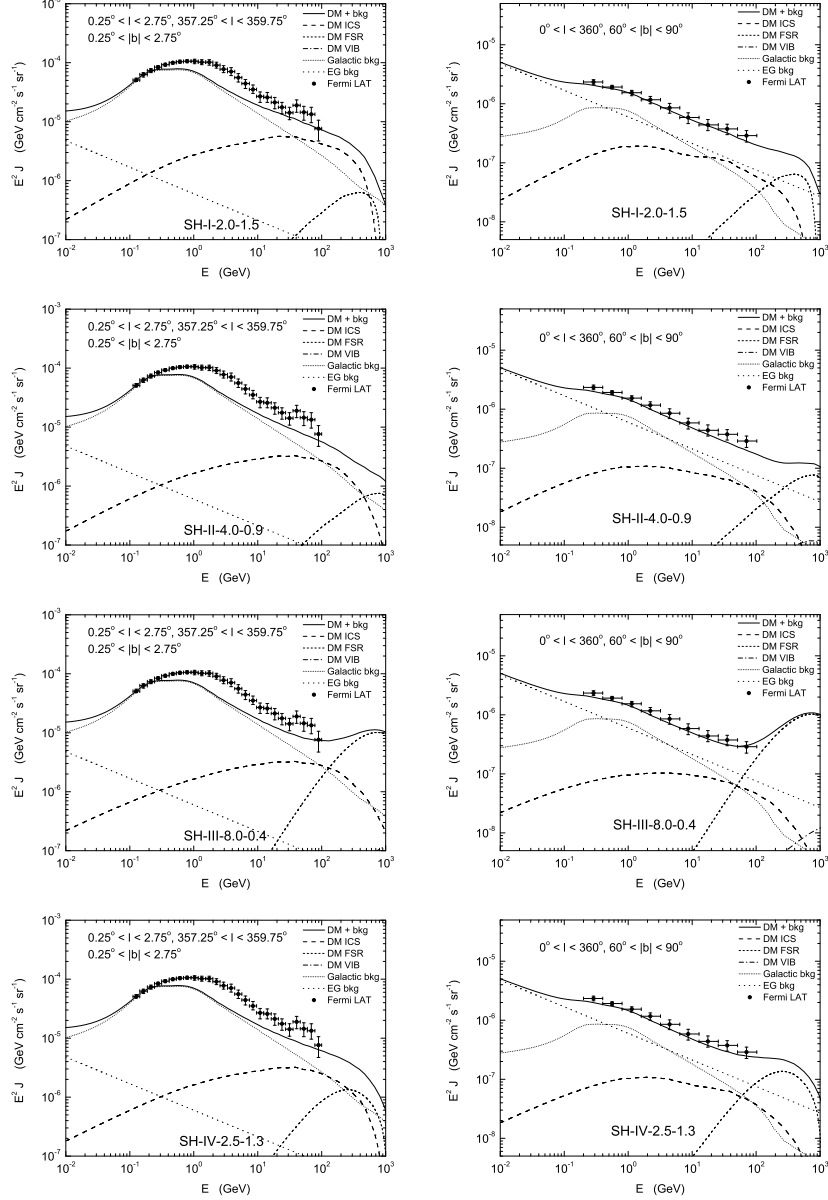


FIG. 9: The predicted gamma-ray spectra for the observed regions  $0.25^\circ < |b| < 2.75^\circ$ ,  $0.25^\circ < |l| < 2.75^\circ$ ,  $357.25^\circ < |b| < 359.75^\circ$  (left) and  $60^\circ < |b| < 90^\circ$ ,  $0^\circ < |l| < 360^\circ$  (right) in the small hierarchy scenario for the cases SH-I  $\sim$  SH-IV.

preliminary results [43]:

$$\Phi_\gamma^{\text{EG}} = 6.0 \times 10^{-7} \left( \frac{E_\gamma}{\text{GeV}} \right)^{-2.45}. \quad (40)$$

In Fig. 8, we show the contributions from ICS, FSR and VIB in various cases in the sky region  $10^\circ < |b| < 20^\circ$ ,  $0^\circ < |l| < 360^\circ$ . For all the cases in lower energy region  $E \lesssim 100$  GeV,

the DM contributions are dominated by the ICS process which is typically 1  $\sim$  2 order of magnitude below the current Fermi-LAT data [43]. The ICS process contributes to a broad spectrum from  $10^{-2}$  GeV to a few hundred GeV. At higher energy region  $E \sim 10 - 100$  GeV, the ICS contribution becomes significant as the background drops rapidly. The ICS has no significant dependence on the mass hierarchy as it only depends on the spectrum of the final state electrons. In general, compared with ICS processes, VIB and FSR contribute to gamma-rays at higher energy. For photon energy above 500 GeV, they become dominant sources and may lead to an up turn of the photon spectrum. This prediction can be tested by the future gamma-ray detectors. The similar conclusions can be obtained for the galactic center region ( $0.25^\circ < |b| < 2.75^\circ$ ,  $0.25^\circ < l < 2.75^\circ$ ,  $357.25^\circ < l < 359.75^\circ$ ) and the galactic pole region ( $60^\circ < |b| < 90^\circ$ ,  $0^\circ < |l| < 360^\circ$ ). As shown in Figs. 8 and 9, the DM particle decay can give significant contributions to the high energy gamma-rays for the three typical regions. For an illustration purpose, we naively sum up the DM contributions (ICS, FSR and VIB) and the diffuse gamma-ray background ( $\Phi_\gamma^{\text{Galactic}}$  and  $\Phi_\gamma^{\text{EG}}$ ). One finds that all the cases are compatible with the current Fermi-LAT preliminary results [43, 44].

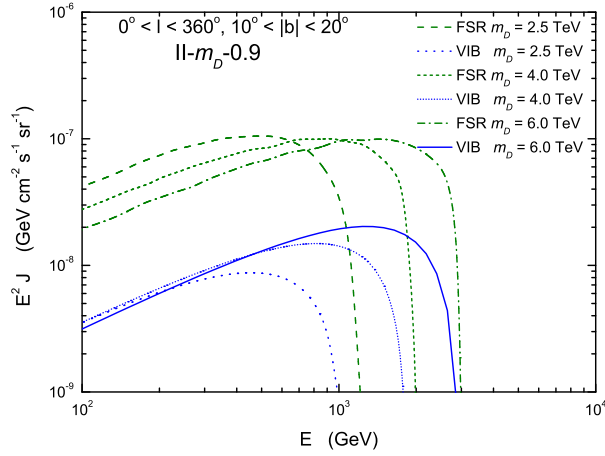


FIG. 10: Comparison of the predicted energy spectra between FSR and VIB process. The curves corresponds to  $S_D = 2.5, 4.0$  and  $6.0$  TeV respectively, with the mass of triplet scalar  $m_{\delta_L}$  fixed at 1 TeV and  $\tau_D = 0.9 \times 10^{26}$ s.

The FSR and VIB processes show stronger dependence on the masses of the triplet scalars, and the two contributions are correlated. It follows from Eq. (15) that for fixed masses of initial DM particle and final states, the decrease of the triplet mass will enhance VIB while slightly suppress FSR. Thus the VIB process can be important for the case with large mass

hierarchy between  $S_D$  and  $\delta_L$ . In Fig. 10, we give the FSR and VIB contributions to the gamma-ray spectrum for three different DM mass cases ( $m_D = 2.5, 4$  and  $6$  TeV). Here we have fixed the triplet mass  $m_{\delta_L} = 1$  TeV and the DM lifetime  $\tau_D = 0.9 \times 10^{26}$  s. We can see that with  $m_D$  increasing, the VIB contribution becomes more significant relative to FSR. For a low  $m_D = 2.5$  TeV, the contribution from VIB relative to that of FSR is only  $\sim 7\%$ . But for a larger  $m_D = 6$  TeV, the contribution can reach  $\sim 20\%$  which is non-negligible.

#### IV. CONCLUSIONS

We have discussed the DM cascade decay induced by tiny soft  $C$ -violating interactions in an extension of a left-right symmetric model in which the DM particle is identified as a gauge singlet scalar. In this scenario, the DM particle may decay favorably into leptonic final states through the intermediate  $SU(2)_L$  triplets. We have explored the parameter space which can well explain the current PAMELA and Fermi-LAT or ATIC experimental data. It is shown that this scenario predicts significant associating signals in the flux of high energy neutrinos and gamma-rays, which is due to the correlated couplings to neutrinos and the extra contributions from the charged components of the triplet. We have found that the predicted neutrino-induced muon flux is dominated by the contribution from the neutrinos directly from the triplet decay. The gamma-ray radiation from the charged triplet scalars through VIB process can be significant in the case that the triplets are much lighter than the DM particle.

#### Acknowledgments

This work is supported in part by the National Basic Research Program of China (973 Program) under Grants No. 2010CB833000; the National Nature Science Foundation of China (NSFC) under Grants No. 10975170, No. 10821504 and No. 10905084; and the Project of Knowledge Innovation Program (PKIP) of the Chinese Academy of Science.

- 
- [1] O. Adriani *et al.* [PAMELA Collaboration], Nature **458**, 607 (2009) [arXiv:0810.4995 [astro-ph]]; Phys. Rev. Lett. **102**, 051101 (2009) [arXiv:0810.4994 [astro-ph]].

- [2] S. W. Barwick *et al.* [HEAT Collaboration], *Astrophys. J.* **482**, L191 (1997) [arXiv:astro-ph/9703192].
- [3] M. Boezio *et al.*, *Astrophys. J.* **532**, 653 (2000).
- [4] M. Aguilar *et al.* [AMS-01 Collaboration], *Phys. Lett. B* **646**, 145 (2007) [arXiv:astro-ph/0703154].
- [5] J. Chang *et al.*, *Nature* **456**, 362 (2008).
- [6] S. Torii *et al.* [PPB-BETS Collaboration], arXiv:0809.0760 [astro-ph].
- [7] A. A. Abdo *et al.* [The Fermi LAT Collaboration], *Phys. Rev. Lett.* **102**, 181101 (2009) [arXiv:0905.0025 [astro-ph.HE]].
- [8] F. Aharonian *et al.* [H.E.S.S. Collaboration], *Phys. Rev. Lett.* **101**, 261104 (2008) [arXiv:0811.3894 [astro-ph]]; arXiv:0905.0105 [astro-ph.HE].
- [9] J. Lavalle, Q. Yuan, D. Maurin and X. J. Bi, *Astron. Astrophys.* **479**, 427 (2008).
- [10] J. Hisano, S. Matsumoto, M. Nagai, O. Saito and M. Senami, *Phys. Lett. B* **646**, 34 (2007) [arXiv:hep-ph/0610249]; M. Cirelli, A. Strumia and M. Tamburini, *Nucl. Phys. B* **787**, 152 (2007) [arXiv:0706.4071 [hep-ph]]; N. Arkani-Hamed, D. P. Finkbeiner, T. R. Slatyer and N. Weiner, *Phys. Rev. D* **79**, 015014 (2009) [arXiv:0810.0713 [hep-ph]]; M. Lattanzi and J. I. Silk, *Phys. Rev. D* **79**, 083523 (2009) [arXiv:0812.0360 [astro-ph]]; M. Backovic and J. P. Ralston, arXiv:0910.1113 [hep-ph]; J. L. Feng, M. Kaplinghat and H. B. Yu, arXiv:0911.0422 [hep-ph]. W. Wang, Z. Xiong, J. M. Yang and L. X. Yu, *JHEP* **0911**, 053 (2009) [arXiv:0908.0486 [hep-ph]].
- [11] D. Feldman, Z. Liu and P. Nath, *Phys. Rev. D* **79**, 063509 (2009) [arXiv:0810.5762 [hep-ph]]; M. Ibe, H. Murayama and T. T. Yanagida, *Phys. Rev. D* **79**, 095009 (2009) [arXiv:0812.0072 [hep-ph]]; W. L. Guo and Y. L. Wu, *Phys. Rev. D* **79**, 055012 (2009) [arXiv:0901.1450 [hep-ph]].
- [12] X. J. Bi, X. G. He and Q. Yuan, *Phys. Lett. B* **678**, 168 (2009) [arXiv:0903.0122 [hep-ph]].
- [13] I. Gogoladze, N. Okada and Q. Shafi, *Phys. Lett. B* **679**, 237 (2009) [arXiv:0904.2201 [hep-ph]].
- [14] C. R. Chen, F. Takahashi and T. T. Yanagida, *Phys. Lett. B* **671**, 71 (2009) [arXiv:0809.0792 [hep-ph]]; C. R. Chen and F. Takahashi, *JCAP* **0902**, 004 (2009) [arXiv:0810.4110 [hep-ph]]; A. E. Nelson and C. Spitzer, arXiv:0810.5167 [hep-ph]; P. f. Yin, Q. Yuan, J. Liu, J. Zhang, X. j. Bi and S. h. Zhu, *Phys. Rev. D* **79**, 023512 (2009) [arXiv:0811.0176 [hep-ph]]; K. Ishiwata, S. Matsumoto and T. Moroi, *Phys. Lett. B* **675**, 446 (2009) [arXiv:0811.0250 [hep-ph]].



- ph]]; A. Ibarra and D. Tran, JCAP **0902**, 021 (2009) [arXiv:0811.1555 [hep-ph]]; A. Arvanitaki, S. Dimopoulos, S. Dubovsky, P. W. Graham, R. Harnik and S. Rajendran, Phys. Rev. D **79**, 105022 (2009) [arXiv:0812.2075 [hep-ph]]; X. J. Bi, P. H. Gu, T. Li and X. Zhang, JHEP **0904**, 103 (2009) [arXiv:0901.0176 [hep-ph]]; C. H. Chen, C. Q. Geng and D. V. Zhuridov, Phys. Lett. B **675**, 77 (2009) [arXiv:0901.2681 [hep-ph]]; S. L. Chen, R. N. Mohapatra, S. Nussinov and Y. Zhang, Phys. Lett. B **677**, 311 (2009) [arXiv:0903.2562 [hep-ph]]. M. Luo, L. Wang, W. Wu and G. Zhu, arXiv:0911.3235 [hep-ph]. J. Zhang, Q. Yuan and X. J. Bi, arXiv:0908.1236 [astro-ph.HE].
- [15] W. L. Guo, L. M. Wang, Y. L. Wu, Y. F. Zhou and C. Zhuang, Phys. Rev. D **79**, 055015 (2009) [arXiv:0811.2556 [hep-ph]].
- [16] Y. L. Wu and Y. F. Zhou, Sci. China **G51**, 1808 (2008) [arXiv:0709.0042 [hep-ph]]. Y. L. Wu and Y. F. Zhou, talk at 4th International Conference on Flavor Physics (ICFP 2007), Beijing, 24-28, Sept, 2007. Int. J. Mod. Phys. A **23**, 3304 (2008) [arXiv:0711.3891 [hep-ph]]; W. l. Guo, L. M. Wang, Y. l. Wu and C. Zhuang, Phys. Rev. D **78**, 035015 (2008) [arXiv:0805.0401 [hep-ph]].
- [17] J. C. Pati and A. Salam, Phys. Rev. D **10**, 275 (1974) [Erratum-ibid. D **11**, 703 (1975)]; R. N. Mohapatra and J. C. Pati, Phys. Rev. D **11**, 566 (1975); G. Senjanovic and R. N. Mohapatra, Phys. Rev. D **12**, 1502 (1975); N. G. Deshpande, J. F. Gunion, B. Kayser and F. I. Olness, Phys. Rev. D **44**, 837 (1991).
- [18] Z. Ahmed *et al.* [The CDMS-II Collaboration and CDMS-II Collaboration], arXiv:0912.3592 [astro-ph.CO].
- [19] T. Bringmann, L. Bergstrom and J. Edsjo, JHEP **0801**, 049 (2008) [arXiv:0710.3169 [hep-ph]].
- [20] A. W. Strong and I. V. Moskalenko, Astrophys. J. **509**, 212 (1998) [arXiv:astro-ph/9807150].
- [21] T. Delahaye, F. Donato, N. Fornengo, J. Lavalle, R. Lineros, P. Salati and R. Taillet, arXiv:0809.5268 [astro-ph].
- [22] D. Maurin, F. Donato, R. Taillet and P. Salati, Astrophys. J. **555**, 585 (2001) [arXiv:astro-ph/0101231].
- [23] T. Delahaye, R. Lineros, F. Donato, N. Fornengo and P. Salati, Phys. Rev. D **77**, 063527 (2008) [arXiv:0712.2312 [astro-ph]].
- [24] E. A. Baltz and J. Edsjo, Phys. Rev. D **59**, 023511 (1998) [arXiv:astro-ph/9808243].
- [25] J. F. Navarro, C. S. Frenk and S. D. M. White, Astrophys. J. **490**, 493 (1997) [arXiv:astro-

- ph/9611107].
- [26] J. N. Bahcall and R. M. Soneira, *Astrophys. J. Suppl.* **44**, 73 (1980).
  - [27] J. Diemand, B. Moore and J. Stadel, *Mon. Not. Roy. Astron. Soc.* **353**, 624 (2004) [arXiv:astro-ph/0402267].
  - [28] J. Hisano, S. Matsumoto, O. Saito and M. Senami, *Phys. Rev. D* **73**, 055004 (2006) [arXiv:hep-ph/0511118].
  - [29] M. Cirelli, M. Kadastik, M. Raidal and A. Strumia, *Nucl. Phys. B* **813**, 1 (2009) [arXiv:0809.2409 [hep-ph]].
  - [30] T. Sjostrand, S. Mrenna and P. Z. Skands, *Comput. Phys. Commun.* **178**, 852 (2008) [arXiv:0710.3820 [hep-ph]].
  - [31] J. Hisano, M. Kawasaki, K. Kohri and K. Nakayama, *Phys. Rev. D* **79**, 043516 (2009) [arXiv:0812.0219 [hep-ph]]; J. Liu, P. f. Yin and S. h. Zhu, arXiv:0812.0964 [astro-ph].
  - [32] A. Strumia and F. Vissani, arXiv:hep-ph/0606054.
  - [33] S. Desai *et al.* [Super-Kamiokande Collaboration], *Phys. Rev. D* **70**, 083523 (2004) [Erratum-ibid. *D* **70**, 109901 (2004)] [arXiv:hep-ex/0404025].
  - [34] J. Mardon, Y. Nomura, D. Stolarski and J. Thaler, *JCAP* **0905**, 016 (2009) [arXiv:0901.2926 [hep-ph]].
  - [35] V. Barger, W. Y. Keung, G. Shaughnessy and A. Tregre, *Phys. Rev. D* **76**, 095008 (2007) [arXiv:0708.1325 [hep-ph]]; C. Delaunay, P. J. Fox and G. Perez, *JHEP* **0905**, 099 (2009) [arXiv:0812.3331 [hep-ph]]; I. Z. Rothstein, T. Schwetz and J. Zupan, *JCAP* **0907**, 018 (2009) [arXiv:0903.3116 [astro-ph.HE]].
  - [36] M. Papucci and A. Strumia, arXiv:0912.0742 [hep-ph]; M. Cirelli, P. Panci and P. D. Serpico, arXiv:0912.0663 [astro-ph.CO].
  - [37] M. Cirelli and P. Panci, *Nucl. Phys. B* **821**, 399 (2009) [arXiv:0904.3830 [astro-ph.CO]].
  - [38] P. Meade, M. Papucci, A. Strumia and T. Volansky, arXiv:0905.0480 [hep-ph].
  - [39] GALPROP Homepage, [http://galprop.stanford.edu/web\\_galprop/galprop\\_home.html](http://galprop.stanford.edu/web_galprop/galprop_home.html); T. A. Porter and A. W. Strong, arXiv:astro-ph/0507119.
  - [40] K. Ishiwata, S. Matsumoto and T. Moroi, *Phys. Lett. B* **679**, 1 (2009) [arXiv:0905.4593 [astro-ph.CO]]; A. Ibarra, D. Tran and C. Weniger, arXiv:0906.1571 [hep-ph]; C. R. Chen, M. M. Nojiri, S. C. Park and J. Shu, arXiv:0908.4317 [hep-ph].
  - [41] M. Regis and P. Ullio, arXiv:0904.4645 [astro-ph.GA]; V. Barger, Y. Gao, W. Y. Keung,

- D. Marfatia and G. Shaughnessy, Phys. Lett. B **678**, 283 (2009) [arXiv:0904.2001 [hep-ph]].
- [42] A. W. Strong, I. V. Moskalenko and O. Reimer, Astrophys. J. **613**, 962 (2004) [arXiv:astro-ph/0406254].
- [43] M. Ackermann, Talk at TeV Particle Astrophysics 2009, <http://www-conf.slac.stanford.edu/tevpa09/Talks.asp>.
- [44] S. Digel, Talk at the 2009 Fermi Symposium, <http://confluence.slac.stanford.edu/display/LSP/FERMI+Symposium+2009>.